Presented at the 32nd European PV Solar Energy Conference and Exhibition, 20-24 June 2016, Munich, Germany

INFLUENCE OF PHOTOVOLTAIC MODULE MOUNTING SYSTEMS ON THE THERMO-MECHANICAL STRESSES IN SOLAR CELLS BY FEM MODELLING

Andreas J. Beinert[1], Matthieu Ebert[1], Ulrich Eitner[1] and Jarir Aktaa[2]
[1] Fraunhofer Institute for Solar Energy Systems ISE, Heidenhofstraße 2, 79110 Freiburg, Germany;
[2] Karlsruhe Institute of Technology (KIT), Hermann-von-Helmholtz-Platz, 76344 Eggenstein-Leopoldshafen, Germany.
Corresponding author: Andreas J. Beinert | Phone: +49 (0)761 4588 5630 | E-mail: Andreas.Beinert@ise.fraunhofer.de

ABSTRACT: The mounting system of photovoltaic (PV) modules has a significant impact on the thermo-mechanical stress in PV modules. In this work the clamping of framed PV modules is compared to the clamping of unframed PV laminates by a simulation study using the finite element method (FEM). The FEM modelling allows to calculate the local stress distribution in the solar cells directly. We present results from a model of a standard glass-backsheet PV module with 3 mm glass under homogenous mechanical pressure load of up to 5400 Pa. The thermal stress from the lamination process is considered as a pre-study, similar to [1]. The frameless clamped PV laminate shows a significantly larger displacement of 147 mm than the framed PV module with 54 mm for 2400 Pa. In line with the findings of Kajari-Schroeder [2] we simulate an elliptic deflection distribution for the framed PV module, whereas the clamped PV laminate shows a wave-like shape. Consequently, the area of high tensile stresses in the silicon solar cells, with a maximum value of 142 MPa at 2400 Pa load, is narrowly located around the highest curvature at the center of the framed PV module. In case of the frameless clamped PV laminate we identify four areas of high tensile stresses with a higher maximum value of 218 MPa. The results show that the frame reduces the tensile stresses in the solar cells significantly compared to unframed laminates.
Keywords: PV Module Design, Thermo-Mechanical Stress, FEM Modelling, Reliability

1 INTRODUCTION

PV module manufactures offer a linear performance warranty of up to 30 years. In order to enable a sufficient service life time, the mechanical stresses in the solar cells have to remain below critical values. A measure for the criticality of stresses is the characteristic fracture stress, at which 63.2% of the solar cells fail. Kaule determined a fracture strength of about 200 MPa [3] for standard solar cells, depending on the orientation. Cracks can cause a significant loss in the module power depending on the type of crack [4]. Hence it is essential to minimize the stress in the solar cells.

1.1 Thermo-mechanical stresses

In PV modules mechanical stresses are induced by mechanical loads, like snow or wind [2], or/and thermally. The latter occur whenever there is a change in temperature of the PV module, starting from the interconnection [5, 6] and lamination process [1] and continuing to the daily and yearly temperature cycles. These stresses are due to the mismatch of the coefficients of thermal expansions (CTE) of the different PV module materials. Often the mechanical stresses which occur in a PV module are a combination of mechanically and thermally induced stresses, hence the terminology thermo-mechanical stresses is used. They are influenced by various factors like the used materials, design and interconnection technique and were investigated thoroughly in the past, e.g. [1, 7]. An overlying effect however is the mounting technology, since it defines the boundary conditions for the module's deformation. In this work we investigate two standard technologies, the clamping of framed and unframed laminates by means of finite element method (FEM) analysis. The aim is to assess the thermo-mechanical stresses in encapsulated solar cells resulting from these systems. For this purpose two three dimensional FEM models of full size PV modules containing 60 solar cells are set up, which differ only in the mounting system. The effect of interconnection techniques is neglected.

2 FINITE ELEMENT MODEL

2.1 Sub-modeling and geometry

The large aspect ratio of the solar module edge length to its thickness demands for high computational effort when using classical continuum mechanics on 3D volumes. Usually plate- or shell-type formulations are used for efficient mechanical modeling of thin structures. However, these descriptions are not designed to describe local stresses in discontinuous layers like the solar cell matrix and are thus not applicable for our purposes. In order to minimize the computational effort of our 3D model, the sub-modeling method is applied in this study. With this method the model is separated in different problems: one for the computation of the displacement, the global model. The second model is a minimized geometry in order to use a finer mesh for the computation of the mechanical stress. This is the so called sub-model.

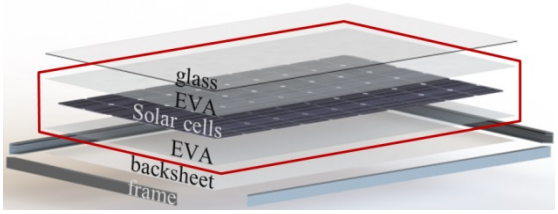

Figure 1: Schematic of a PV laminate with a frame, which is implemented as a sub-model in the FEM model. The red box indicates the sub-model for stress analysis.

The global model consists of the PV laminate, as shown schematically in figure 1, without any mounting system. By exploiting the symmetry of a PV module, a quarter of the PV laminate containing 15 solar cells is modelled. The corresponding materials and layer thicknesses are given in table I. The mounting system is implemented as another fully coupled sub-model to the laminate. Thus the laminate could be meshed identically in both FEM models.

Table I: Materials of the PV laminate used in the FEM model with the applied material model and thickness.

Layer	Material	Material model	Thickness [µm]
Front Glass	solar glass	linear elastic	3000
Encapsulant	EVA	linear elastic	400
Solar Cells	monocrystalline silicon	linear elastic, anisotropic	200
Backsheet	PVF-PET-PVF	linear elastic	350

In the sub-model for the stress computation the laminate is reduced to the solar cell matrix embedded in the encapsulant, as indicated by the red box in figure 1. The deformation of the sub-model is given from the global model on the boundary encapsulant/glass and encapsulant/backsheet.

2.2 Materials and mesh

The solar cells are modelled as full-square monocrystalline silicon cells without any metallization. This allows for the use of rectangular mesh elements. The global model exhibits 7.7×10^6 and the sub-model 18.6×10^6 degrees of freedom. Figure 2 shows the cross section of the aluminum frame and the aluminum laminate clamp. Sliding at the interface is prohibited and the displacement field is continuous. The rubber inlay is meshed with a finer resolution.

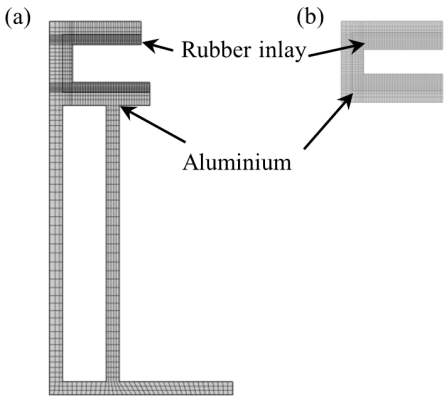

Figure 2: Cross section of the meshed aluminum frame (a) and the aluminum laminate clamp (b) with a finer meshed rubber inlay.

For all materials linear elastic material models are used. The corresponding material parameters are given in table II. Instead of modeling the full viscoelastic behavior of EVA [8] we take into account only the temperature dependency by using a function of T for the Young's modulus. The monocrystallinity of silicon is modelled by a cubic-symmetric elasticity matrix given in [1].

The computation itself is carried out in two successive steps. First the lamination process is modeled by cooling down from a stress-free state at 150°C to 25°C. In this step the mounting structure is not considered. Secondly the mechanical load test at room temperature is applied onto the thermally stressed module. According to the IEC 61215 [9] the glass surface is homogenously loaded with 2400 Pa and 5400 Pa. The mounting of the frame and the clamp is modelled by a fixed constraint, with a distance of 20% of the PV module length from the short edge. This boundary condition represents the screwing on a rack and is comparable to model 8 in the study of Schicker [10].

Table II: Material properties used in the FEM model; *: provided by manufacturer.

Material	Density ρ [kg/m³]	Young's modulus E [GPa]	Poisson's ratio ν [-]	CTE α [10^{-6} K^{-1}]
Glass [11]	2500	70	0.2	9
EVA [7]	960	T-dep.	0.4	270
Silicon [1, 12, 13]	2329	elasticity matrix		T-dep.
Back Sheet [1]	2520	3.5	0.29	50.4
Aluminum [14]	2700	70	0.33	23
Rubber inlay*	67	0.0074	0.3	769

3 RESULTS

3.1 Lamination

The compression due to the cooling down process after lamination is shown in figure 3. A maximum compressive stress of 81 MPa is obtained on the rear surface of the solar cells. The compressive stresses show a superposition of the compression of the laminate and the solar cells themselves. Therefore the compressive stress is slightly higher at the edge of the laminate than in the center. Since compressive stress is less crucial for silicon solar cells than tensile stress, the stress obtained from lamination is not critical. In the encapsulant no significant stresses are obtained, which reflects the buffering character of EVA.

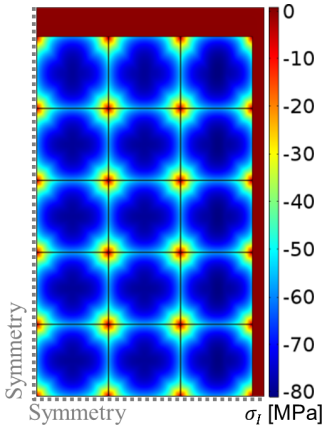

Figure 3: Thermal compression stress from lamination process on the rear surface of the solar cell layer. The color table shows the third principal stress σ_{III}. The dotted line represents the symmetry plane.

3.2 Mechanical load of 2400 Pa

In this section the results of the FEM model for the mechanical pressure load test with 2400 Pa are presented. Since the distribution at 5400 Pa is very similar, only the maximum values are shown in figure 6.

Figure 4 shows the total displacement d at 2400 Pa homogeneous mechanical pressure load on a glass-backsheet PV laminate mounted with four aluminum clamps (b) and the same PV laminate with a frame mounted on a rack (a). The corresponding maximum values are given in figure 6 (left). With a maximum displacement of 54 mm the framed PV module shows a much smaller displacement compared to the maximum displacement of 147 mm of the frameless PV laminate mounted by four clamps. The displacement of the frameless laminate is a superposition of a deflection in x-direction and a deflection in y-direction. It exhibits a wave like character, while the framed PV module shows an elliptic distribution. The different deflection shape arises from the additional stiffness which the frame provides to the laminate. The frame supports the PV laminate along all four edges while the clamps support the module locally at four positions. Therefore the displacement at the edges almost vanishes for the framed PV module, while the frameless PV laminate shows a significant displacement between the clamps.

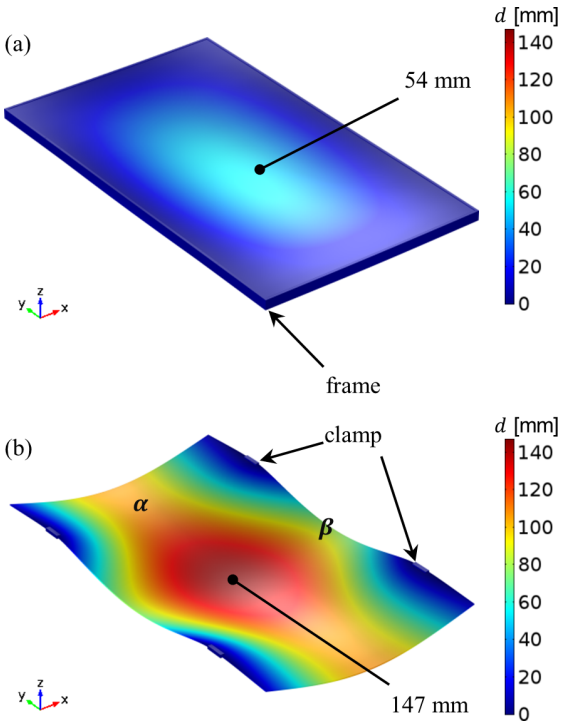

Figure 4: Total displacement d from homogenous mechanical load with 2400 Pa for the full framed PV module (a) and full unframed PV laminate mounted with clamps (b). The color legend shows the displacement values in mm. The displacement is represented by the deformation of the geometry (to scale).

Due to the deflection, the highest tensile stresses in the solar cells occur on their rear side. The distribution of the first principal stress σ_I on the rear side of the solar cells at 2400 Pa is shown in figure 5. The maximum values are depicted in the right part of figure 6. For the framed module the maximum value of 142 MPa is below the fracture strength of 197 MPa [3]. Therefore no significant cell breakage is expected for framed modules. For unframed modules the fracture strength is exceeded in 16 of the 60 cells with a maximum of 218 MPa, as indicated by the dashed ellipse in figure 5. Hence we expect a critical risk of cracks for unframed glass-backsheet modules.

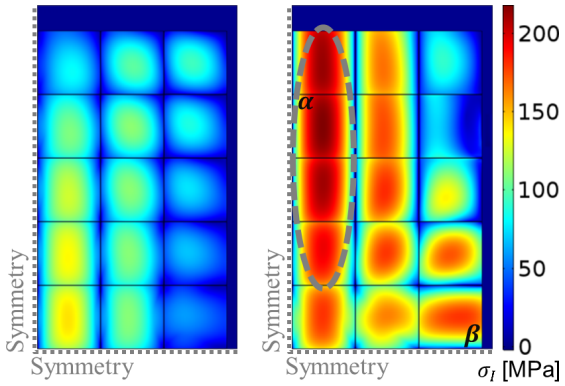

Figure 5: Tensile stress on the rear side of the solar cells resulting from homogenous mechanical load with 2400 Pa for the framed PV module (left) and the unframed laminate mounted with clamps (right). The color legend shows the first principal stress σ_I and the dashed ellipse indicates cells with stress values above the fracture strength reported in [3].

The stress distribution in the solar cells corresponds to the different displacement shapes seen in figure 4. For the homogenous displacement distribution of the framed PV module, the maximum curvature occurs at the maximum deflection in the center of the PV module. Hence the highest tensile stress in the solar cells is found at the symmetry corner of the framed PV module. The stresses in the module corner arise from high diagonal strains, as described in [2]. Contrary in the case of the frameless PV module: due to the sinus-like deflection, the maximum curvature does not occur at the maximum deflection. Additional to the global maximum in the module center, we find two local maxima, which are marked by "α" and "β" respectively in figure 4. These correspond to the deflections in x- and y-direction. At these local maxima, the principal stress directions are dominated by the resulting curvature. Therefore two areas of high tensile stresses occur in the solar cells. Consequently, the overall area of high tensile stresses is larger for unframed laminates than for framed modules.

3.2 Mechanical load of 5400 Pa

With increasing load the deflection increases and hence the difference in the deflection shape becomes more crucial. According to the FEM results of 5400 Pa load, 52 of the 60 solar cells in the unframed, clamped PV laminate are exposed to tensile stresses above the fracture strength with a maximum of 443 MPa. Consequently a severe cell breakage is anticipated at high loads for clamped PV laminates. Also in the framed PV module the fracture strength is exceeded with a maximum tensile stress value of 268 MPa at 5400 Pa load. However only 12 of the 60 cells show tensile stresses above the fracture strength. Hence cell cracking is expected to a less extend than for the frameless laminate. By increasing the glass stiffness, i.e. increasing

the thickness and/or the Young's modulus, the stress values will decrease. For framed modules the frame geometry can be optimized additionally. With these measures the tensile stresses in framed PV modules could be decreased below the fracture strength given in [3]. The tensile stresses in frameless glass-backsheet laminates can hardly be decreased below the fracture strength. Therefore glass-glass PV laminates should be investigated for heavy loads.

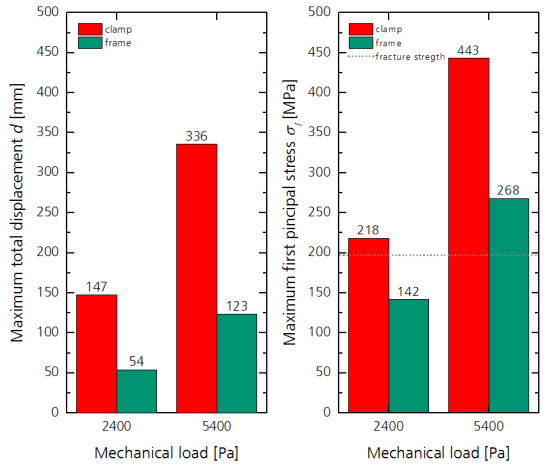

Figure 6: Total displacement d (left) and first principal stress σ_I (right) depending on applied mechanical load.

4 CONCLUSION AND OUTLOOK

A simulation model for a straightforward thermo-mechanical assessment of different mounting systems is presented. In this study the clamping of framed and unframed glass-backsheet PV modules is compared by FEM modelling in regards to the mechanical stress in the solar cells due to mechanical load from the glass side.

The deflection shape of the two concepts shows a different pattern. Due to supporting at four local positions, the unframed laminate has a wave-like deflection. The support which the frame provides to the laminate along all edges leads to an elliptic deflection. Consequently the area of high tensile stresses is larger in frameless PV laminates compared to framed PV modules.

With 142 MPa compared to 218 MPa at 2400 Pa mechanical load, the results show significantly higher tensile stresses in the cells for the clamping of unframed PV laminates compared to clamped framed PV modules. With 16 of 60 solar cells showing tensile stresses above the fracture strength given in [3], it is most likely that cell cracking will occur for the clamping of unframed laminates. At the same load level, the stresses in a framed module are well below the fracture strength. Therefore the stiffness provided by the frame is sufficient to avoid cell cracking at a load of 2400 Pa.

At a load of 5400 Pa tensile stresses above the fracture strength arise in both concepts. With 52 of the 60 solar cells in the clamped laminate showing critical stress values, severe cell cracking is expected. This is reduced by the frame to 12 out of 60 cells with significantly lower maximum values of 268 MPa compared to 443 MPa. A further stress reduction can be achieved by replacing the backsheet with an additional glass. This will be investigated by the presented model in the future. Also further mounting technologies as well as PV module concepts can easily be investigated.

The presented results prove that, from a mechanical point of view, a frame is essential for glass-backsheet laminates.

5 REFERENCES

[1] U. Eitner, S. Kajari-Schroeder, M. Koentges, and H. Altenbach, "Thermal stress and strain of solar cells in photovoltaic modules," in *Advanced Structured Materials*, vol. 15, *Shell-like Structures: Non-classical Theories and Applications*, H. Altenbach and V. A. Eremeyev, Eds, Berlin/Heidelberg: Springer, 2011.

[2] S. Kajari-Schröder, I. Kunze, U. Eitner, and M. Koentges, "Spatial and orientational distribution of cracks in crystalline photovoltaic modules generated by mechanical load tests," *Solar Energy Materials and Solar Cells*, vol. 95, no. 11, pp. 3054–3059, 2011.

[3] F. Kaule, W. Wang, and S. Schoenfelder, "Modeling and testing the mechanical strength of solar cells," *Solar Energy Materials and Solar Cells*, vol. 120, Part A, pp. 441–447, 2014.

[4] S. Kajari-Schröder, I. Kunze, and M. Köntges, "Criticality of cracks in PV modules," *Energy Procedia*, vol. 27, pp. 658–663, 2012.

[5] J. Wendt, M. Träger, M. Mette, A. Pfennig, and B. Jäckel, "The link between mechanical stress induced by soldering and micro damages in silicon solar cells," in *Proc. of the 24th EUPVSEC*, 2009, pp. 2705–2708.

[6] B. Lalaguna, P. Sánchez-Friera, H. Mäckel, D. Sánchez, and J. Alonso, "Evaluation of stress on cells during different interconnection processes," in *Proc. of the 23rd EUPVSEC*, 2008, pp. 2705–2708.

[7] U. Eitner, "Thermomechanics of photovoltaic modules," Dissertation, Zentrum für Ingenieurwissenschaften, Halle-Wittenberg, Martin-Luther-Universität, Halle, 2011.

[8] U. Eitner, S. Kajari-Schröder, M. Köntges, and R. Brendel, "Non-Linear Mechanical Properties of Ethylene-Vinyl Acetate (EVA) and its Relevance to Thermomechanics of Photovoltaic Modules," in *Proc. of the 25th EUPVSEC/ 5th World Conference on Energy Conversion*, 2010, pp. 4366–4368.

[9] *IEC 61215: 2005-04. Crystalline silicon terrestrial photovoltaic (PV) modules - Design qualification and type approval*, 2005.

[10] J. Schicker, C. Hirschl, and R. Leidl, "Effect of PV Module Frame Boundaries on Stresses in Solar Cells," *Journal of Energy Challenges & Mechanics*, vol. 1, no. 3, pp. 155–162, 2014.

[11] f|solar, *data sheet f | solarfloat*. Sülzetal: f | solar GmbH.

[12] R. B. Roberts, "Thermal expansion reference data: silicon 300-850 K," *Journal of Physics D: Applied Physics*, vol. 14, no. 10, pp. L163, 1981.

[13] R. B. Roberts, "Thermal expansion reference data: silicon 80-280K," *Journal of Physics D: Applied Physics*, vol. 15, no. 9, pp. L119, 1982.

[14] W. M. Haynes, *CRC handbook of chemistry and physics*: CRC press, 2014.